Scientific Reports

https://doi.org/10.1038/s41598-026-40477-8

Article in Press

Using deep learning to explore the impacts of street-view green space on school myopia prevalence: a multicenter, cross-sectional study

Received: 16 November 2025

Accepted: 13 February 2026

Published online: 25 February 2026

Cite this article as: Hua D., Yang T., Cui Q. *et al.* Using deep learning to explore the impacts of street-view green space on school myopia prevalence: a multicenter, cross-sectional study. *Sci Rep* (2026). https://doi.org/10.1038/s41598-026-40477-8

Dihao Hua, Tianshu Yang, Qi Cui, Jian Zhang, Gang Luo, Anshun Cheng, Wu'an Su, Mei Ming, Fangyuan Zhou, Ruoyu Zhang, Zhendong Yuan, Changzheng Chen, Yishuang Xu & Zhen Chen

Using deep learning to explore the impacts of street-view green space on school myopia prevalence: a multicenter, cross-sectional study

Ph.D. Dihao Hua[1#], Email: dihaohuaphd@163.com

Mr. Tianshu Yang[1#], Email: tianshuyang@whu.edu.cn

Mr. Qi Cui[2#], Email: qicuisgg@whu.edu.cn

Dr. Jian Zhang[3#], Email: zhj2208@sina.com

Dr. Gang Luo[5], Email: 289686915@qq.com

Dr. Anshun Cheng[5], Email: 403338853@qq.com

Dr. Wu'an Su[6], Email: 123443434@qq.com

Dr. Mei Ming[4], Email: 276949485@qq.com

Ms. Fangyuan Zhou[1], Email: fyyy0823@whu.edu.cn

Ms. Ruoyu Zhang[1], Email: 2038928968@qq.com

Ph.D Zhendong yuan[7*], Email: z.yuan@uu.nl

Prof. Changzheng Chen[1*], Email: whuchenchzh@163.com

Dr. Yishuang Xu[1*], Email: 540282252@qq.com

Prof. Zhen Chen[1*], Email: hchenzhen@163.com

[1] Department of Ophthalmology, Renmin Hospital of Wuhan University, 430060 Wuhan, Hubei; China

[2] Yunnan Province Surveying and Mapping Data Archives, Kunming, Yunnan; China

[3] Department of Ophthalmology, Ezhou Center Hospital, Ezhou, Hubei; China

[4] Department of Ophthalmology, Huangshi Central Hospital, Huangshi, Hubei, China

[5] Department of Ophthalmology, Enshi Huiyi Eye Hospital, Enshi, Hubei, China

[6] Department of Ophthalmology, Kang Ze Eye Hospital, Jingmen, Hubei, China
[7] Institute for Risk Assessment Sciences, Utrecht University, Utrecht, the Netherlands

#Dihao Hua, Tianshu Yang, Qi Cui and Zhang Jian contributed equally to this work.
*Corresponding Author: Zhendong yuan, Changzheng Chen, Yishuang Xu and Zhen Chen

Abstract
Background: Previous studies used the Normalized Difference Vegetation Index (NDVI) to assess green space and showed its potential protective effect on myopia. However, this top-down measurement of green space cannot fully reflect the eye-level greenness perception. This study used the Vision Greenness Index (VGI) to assess visual greenness from street-view images and compare its effect on myopia with NDVI.
Methods: This multicenter, cross-sectional study investigated 69,051 children from 146 schools in five cities in Hubei, ranging from kindergarten to high school. Visual greenness was calculated from street-view images with DeepLab v3 and NDVI was calculated from Landsat 8 satellite observations. Regression models were used to analyze the relationship between school myopia and environmental factors.
Results: The partial correlation coefficient between VGI within a 5,000-m buffer zone and myopia was -0.343 (P = 0.038) and -0.326 (P < 0.001) in Models 1 (all schools) and 2 (schools except high

schools), respectively, whereas NDVI showed no significant results. In Model 3 (kindergartens), the partial correlation coefficients between VGI and NDVI within a 5,000-m buffer zone were -0.675 (P = 0.029) and -0.380 (P = 0.032), respectively. In Model 4 (elementary schools), the partial correlation coefficients between VGI and NVDI within a 5,000-m buffer zone were -0.310 (P = 0.027) and -0.088 (P = 0.043), respectively. Model 5 (high schools) did not demonstrate any correlations between the identified factors and the prevalence of myopia during high school.
Conclusions: VGI demonstrated a more significant relation to the myopia than NVDI. Visual greenness was found to be related to myopia in kindergartens and elementary schools rather than in high school, indicating its more significant association with a lower prevalence of myopia in early school ages than in high school.
Keywords: School myopia, Normalized difference vegetation index, Vision greenness index, Street-view green space

1. Introduction

Myopia is a common cause of visual impairment. It is increasingly becoming a global health issue with significant economic implications (1). Epidemiologic data estimates that people with myopia will comprise 49.8% of the global population by 2050 (2). Myopic children in early school ages may face a relatively high risk of progressing to high myopia (3). High myopia is associated with several sequelae, such as retinal detachment, glaucoma, and myopia-associated retinopathy (4, 5). Myopia has placed an estimated economic burden of 26.3 billion US dollars on China (6). Comprehensive myopia control has the potential to reduce this

burden, particularly when implemented during school age when myopia rates rise rapidly (7, 8). The question remains about how to make strategies for school myopia prevention more effective and cost-saving.

Myopia develops from an interplay of hereditary and behavioral factors, as factors proven to be associated with myopia include genetics, increasing near work owing to high educational stress, and low time outdoors (9). Environmental factors, such as duration of natural daylight, amount of green space, and degree of air pollution, also proved by clinical investigations to be associated with the prevalence of myopia (10-13). Controlling these environmental risk factors may reduce the incidence of myopia. Given students spend significant time in school, how the school environment and green space impact school myopia prevention is understudied. For instance, a Beijing study reported that a 500-meter radius of green space around schools seemed to delay the onset of myopia (14). However, a similar protective effect required a 1,000-m radius of green space in Tianjin (15). The environment varies across regions, making comprehensive research on the school environment and myopia in each region needed to advise local myopia prevention. Given that Chinese students spend much time in school, the school environment serves as an important exposure domain for both daily activities and intensive near-work. Myopia prevalence and its progression rates vary significantly across academic stages (16). Different grade students are facing rising academic pressure and decreasing outdoor time, which may lead to different effects of the school environment on myopia across

grades (17). Thus, research on the school environment and myopia needs to employ a stratified approach to capture these grade-specific differences.

In the literature, green space is identified as a protective environmental factor against diseases like mental illness, cardiovascular disease, and myopia (13, 18, 19). Previous myopia studies used remote sensing technology to show that larger size and better morphology of green space were associated with a reduced risk of school myopia, which may be derived from more outdoor activity, lower near work time, and reduced air pollution related to green space (20-22). Satellite images were used in these studies to calculate the Normalized Difference Vegetation Index (NDVI), which mainly reflects the overall coverage of green space (23). In contrast, using deep learning methods, the Vision Greenness Index (VGI) derived from semantic segmentation of street-view images provides a more accurate reflection of eye-level greenness compared to NDVI (24-26). Intuitively, this eye-level greenness is more aligned with human perception. Studies show that VGI exhibits a protective effect against depression and cardiovascular diseases, lacking evidence about the relationship between VGI and myopia (27, 28). Comparison between NDVI and VGI in the myopia study may provide a clearer picture of the effect of green spaces on the prevalence of myopia.

This study investigated 69,051 students from 146 schools in five cities of Hubei Province in 2022. Using regression analysis, we examined the relationship of environmental factors on myopia and

compared the correlation between VGI and NDVI with the prevalence of myopia in schools, aiming to explore whether the street view green space index can better represent greenness exposure in myopia studies than satellite products and enhance understanding about how the school environment is associated with myopia prevalence.

2. Materials and Methods

2.1 Study design

This was a multicenter, cross-sectional study approved by the Ethics Committee of Renmin Hospital of Wuhan University (WDRY2020-K234) and followed the tenets of the Declaration of Helsinki. Informed consent was obtained from all the subjects in this study. For all minor participants, informed consent was obtained from a parent and/or legal guardian.

Participants were from 146 schools in the Wuhan, Ezhou, Huangshi, Jingmen, and Enshi cities of Hubei Province in 2022. The schools included kindergartens, elementary schools, junior high schools, and senior high schools. All participants underwent an eye examination, which included visual acuity testing, refraction, and slit-lamp biomicroscope. Uncorrected visual acuity was assessed for each eye using the tumbling E Early Treatment Diabetic Retinopathy Study charts at a distance of 4 meters in a well-lit indoor area. Non-cycloplegic refraction was performed using a fully automatic computer optometer (RM800; TOPCON, Tokyo, Japan) and subjectively refined by well-trained optometrists. Slit-lamp

biomicroscope of the anterior segment was performed by the same optometrists.

According to the International Myopia Institute Defining and Classifying Myopia Report, myopia was diagnosed in all participants with the spherical equivalent refractive error of an eye is ≤ –0.5 D (29). Exclusion criteria included: (1) age < 4-years or > 19-years; (2) best corrected visual acuity < 1.0; (3) history of strabismus surgery or intraocular surgery; (4) history of glaucoma, intraocular inflammation, intraocular media opacifications, or retinal disease; and (5) history of neurodegenerative diseases.

2.2 Street view variables

Based on OpenStreetMap, we constructed the road network of Hubei Province and divided it into road segments. Sampling points were taken at 100-m intervals along each road within a 5-kilometer radius around the schools. Street view images were obtained at these sampling points using Baidu Maps' Street View Service (https://api.map.baidu.com/). Four images taken from different angles (0°, 90°, 180°, and 270°) were collected for each sample point. Street view images used in our study were taken in 2022 to match the participants' condition. A total of 60,995 street-view images were obtained.

Deep learning was employed for image segmentation to optimize previous pixel-based classification methods, which cannot differentiate between natural and artificial green objects. DeepLab v3 semantic segmentation was used to accurately identify the

green spaces in our street view images. The Xception network from DeepLab v3 is a form of depth-wise separable convolution that decomposes a standard convolution into smaller operations and serves as our backbone architecture. This architecture significantly reduces computational complexity and improves performance. DeepLab v3 also incorporates dilated convolutions and Atrous Spatial Pyramid Pooling (ASPP), which allows convolutional operations to capture contextual information on multiple scales and extract richer feature information. The ASPP module captures multi-scale contextual information by applying parallel atrous convolutions with different rates. Its output is expressed as:

$$y = \text{Concat}(y_1, y_2, y_3, y_4)$$

Where: (y_1, y_2, y_3, y_4) are the outputs of atrous convolutions with different rates, Concat denotes the concatenation operation of feature maps.

The convolutional layers extract features from the input street view images, whereas pooling layers compress the data to learn higher-level feature maps, which reduces spatial dimensions. DeepLab v3 then uses cross-entropy to adjust the parameters of each layer, iterating through multiple rounds of training to obtain a high-accuracy semantic segmentation network. DeepLab V3 also employs a cross-entropy loss function, defined as:

$$L = -\sum_{i}\sum_{c} y_{i,c} \log(p_{i,c})$$

Where: $y_{i,c}$ is the ground truth label for pixel i. $p_{i,c}$ is the predicted probability of pixel i belonging to class c.

We trained our model using a set of annotated images from the ADE20K database, which contains a large number and range of labeled object categories, like cars and trees (30). This model was trained to identify greenness based on morphological and structural features of true vegetation (e.g., trees, grass, plants), rather than just green pixels. By feeding street view images into the trained network, we obtained the segmentation results, which were then used to calculate the proportion of green space. The green space ratio for each sampling point was computed by calculating the ratio of green space pixels to total image pixels. The green space ratio for each point was then averaged from the four cardinal directions to obtain the overall vision greenness index (VGI) for that point. Three buffer zones of VGI were established with radii of 1,000-m, 3,000-m, and 5,000-m. VGI with different buffer zones was calculated from 3512 street-view images in 1,000-m buffer zone, 21018 street-view images in 3,000-m buffer zone and 60995 street-view images in 5,000-m buffer zone, respectively. VGI values range between 0 and 1, with higher values indicating a greater proportion of visual greenness.

2.3 Remote sensing variables

The difference in green space between street view images and remote sensing images is shown in Figure 1. To compare with the street-level greenness index, we obtained remote sensing images of Hubei using the Landsat 8 satellite data from the U.S. Geological Survey database, with a spatial resolution of 30 meters. These images were accessible via USGS Earth Explorer (https://earthexplorer.usgs.gov/). NDVI was calculated within a

circular buffer zone for each school using QGIS software (https://qgis.org/en/site/forusers/download.html, version 3.34.8) derived from Landsat 8 imagery acquired between June and September in 2022. This period was selected for optimal data availability and seasonal foliation characteristics within the study region. The NDVI estimates green exposure in remote sensing images by measuring the differences in the reflectivity of light. Cloud and cloud-shadow pixels were masked using the quality assurance band. NDVI was computed for each available scene, and the mean value was used for seasonal compositing to reduce noise and residual cloud contamination associated with single-date imagery. Buffer zones of NDVI were established with radii of 1,000-m, 3,000-m, and 5,000-m to compare their relation to myopia with VGI. NDVI values fall between -1 and 1, with higher values indicating greater vegetation. NDVI was calculated as follows:

$$NDVI = \frac{NIR - Red}{NIR + Red}$$

Where: NIR refers to the reflectance in the near-infrared region of the electromagnetic spectrum, and Red refers to the reflectance in the visible red region.

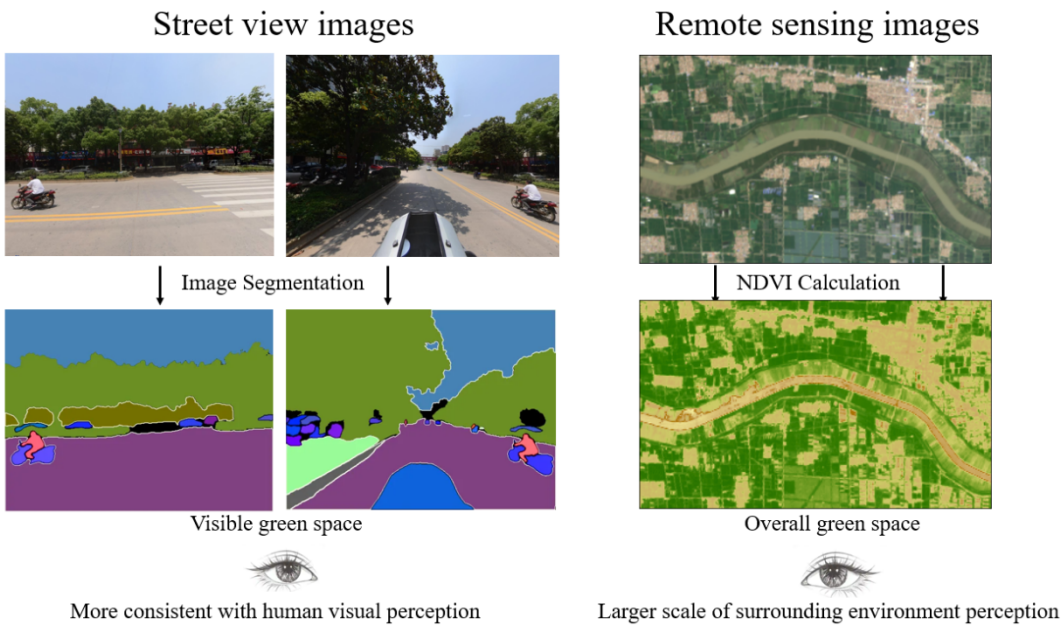

Figure 1. Differences between Street-view Green Space and NDVI. The remote sensing imagery was derived from Landsat 8 data accessed via the USGS EarthExplorer website at https://earthexplorer.usgs.gov/. The NDVI calculations were performed using QGIS software (Version 3.34.8, available at https://qgis.org/en/site/forusers/download.html). NDVI: Normalized Difference Vegetation Index

2.4 Environmental variables

Myopia is also related to other environmental variables, including air pollution, climatic factors, and physical activity levels (13). We utilized air pollution data from the Department of Ecology and Environment of Hubei Province (https://sthjt.hubei.gov.cn/hjsj/) to calculate the average annual levels of carbon monoxide (CO), sulfur dioxide (SO_2), nitrogen dioxide (NO_2), ozone (O_3), and particulate matter with a diameter less than or equal to 2.5 micrometers (PM2.5) around each school. We also obtained select meteorological monitoring data from the Hubei Provincial

Meteorological Monitoring Station (https://data.cma.cn/dataService/) to calculate the annual average sunshine hours, temperature, and rainfall levels around each school. For monitoring station data, school-level exposure estimates were obtained using kriging interpolation. Sports areas around each school were identified using Baidu Maps API (https://api.map.baidu.com/). We invoked the Baidu Maps POI API to retrieve all POIs tagged as sports venues, playgrounds, fitness facilities, etc. Duplicate records with identical names and coordinates were removed, then point POIs were converted to density counts and polygon features were summed for their actual areas.

2.5 Statistical analyses

After data processing, non-parametric Spearman correlation analysis was used to assess the associations between the exposure factors. Variance inflation factor (VIF) was used to evaluate multicollinearity among variables, with this value greater than 3 suggesting problematic. Standard diagnostics revealed no violations of linear regression assumptions. Based on our linear regression models, the prevalence rate was set as the outcome variable, with VGI, NDVI, and other environmental variables categorized as exposure factors. The partial correlation coefficient represented the unbiased correlation between the specific exposure factors and the outcome variable after controlling for other environmental variables. Models were stratified by school types and fitted for all schools (Model 1) and schools excluding high schools (Model 2), kindergarten (Model 3), elementary schools

(Model 4), and high schools (Model 5). Model performance was assessed using the Akaike Information Criterion (AIC), with lower AIC values indicating better model fit (29). Our analysis was performed using complete case data without imputation for missing data and dropouts. Two-sided p-values of less than 0.05 were considered statistically significant. RStudio for Windows (V4.2.3. Boston, MA, USA) was used for data analysis.

3. Results

3.1 Study population

A total of 71,302 students (33,800 boys and 37,502 girls) were included in this study in the year 2022. Forty-six students (22 boys and 24 girls) were excluded because of previous eye surgery, whereas 1,079 students (535 boys and 544 girls) were excluded because their best-corrected visual acuity was lower than 1.0. Another 1,126 students (680 boys and 446 girls) were excluded because the remote sensing images of their schools were severely obstructed. The remaining 69,051 students (32,563 boys and 36,488 girls) comprised the study population.

Table 1 describes the demographic data of all schools. Overall, the average age of the students was 11.8 years, with 59.9% having myopia and 50.3% being female. Among the students, 8.9% were in kindergarten, 43.2% were in elementary school, 28.9% were in junior high school, and 19% were in senior high school. Figure 3 describes the myopia rates in all school levels. As shown in Figure 2, the prevalence of myopia reached a minor peak during the third year of kindergarten and continued to increase steadily throughout

elementary school, with a rapid rise during the third grade. Prevalence rates grew steadily through junior and senior high school.

Table 1. Demographic data of all schools

□	Proportion/ (%)	Population
Education Stage: Kindergarten	8.9	6191
Elementary schools	43.2	29841
Junior high schools	28.9	20016
Senior high schools	19	13003
Myopia: Myopia	59.9	41339
Non-myopia	41.1	27712
Gender: Male	49.7	32563
Female	50.3	36488

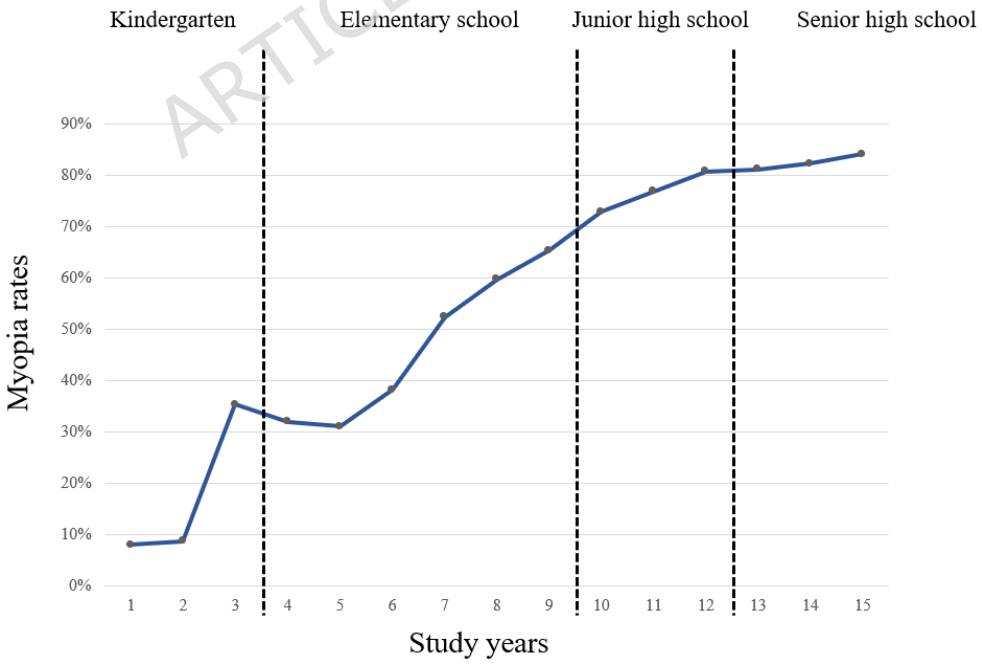

Figure 2. Myopia rate in different school levels

Table 2 describes the characteristics of the areas surrounding the schools. Three different street view radii were chosen. Data processing and visualization followed standard protocols for remote sensing analysis. Figure 3 shows the locations of the included schools.

Table 2. Characteristics of the school environments and school myopia.

□	Min.	Mean (SD)	Max.
VGI: 1,000-m buffer	0.01	0.10(0.06)	0.22
3,000-m buffer	0.01	0.11(0.07)	0.27
5,000-m buffer	0.01	0.15(0.06)	0.28
NDVI: 1,000-m buffer	-0.02	0.32(0.14)	0.54
3,000-m buffer	0.04	0.31(0.15)	0.54
5,000-m buffer	0.10	0.31(0.12)	0.54
Carbon monoxide (ug/m^3)	63.1	84.4(9.3)	104.7
Particulate matter 2.5 (ug/m^3)	24.5	60.1(11.2)	125.4
Sulfur dioxide (ug/m^3)	32.1	40.3(8.7)	90.5
Nitrogen dioxide (ug/m^3)	10.8	42.4(4.3)	70.5
Ozone (ug/m^3)	40.1	64.2(9.6)	90.6
Sunshine hours (h/day)	4.26	4.5(0.1)	4.79
Temperature (℃/day)	16.8	17.0(0.1)	17.3
Rainfall (mm/day)	2.3	2.5(0.1)	2.8
Sports area (m^2)	0.4	47.6(31.7)	99.7
Age (years)	4	11.8(3.8)	19
Prescription for the left eye	3.3	4.54(0.33)	5.0
Prescription for the right eye	3.3	4.57(0.33)	5.0

VGI: Vision Greenness Index; NDVI: Normalized Difference Vegetation Index.

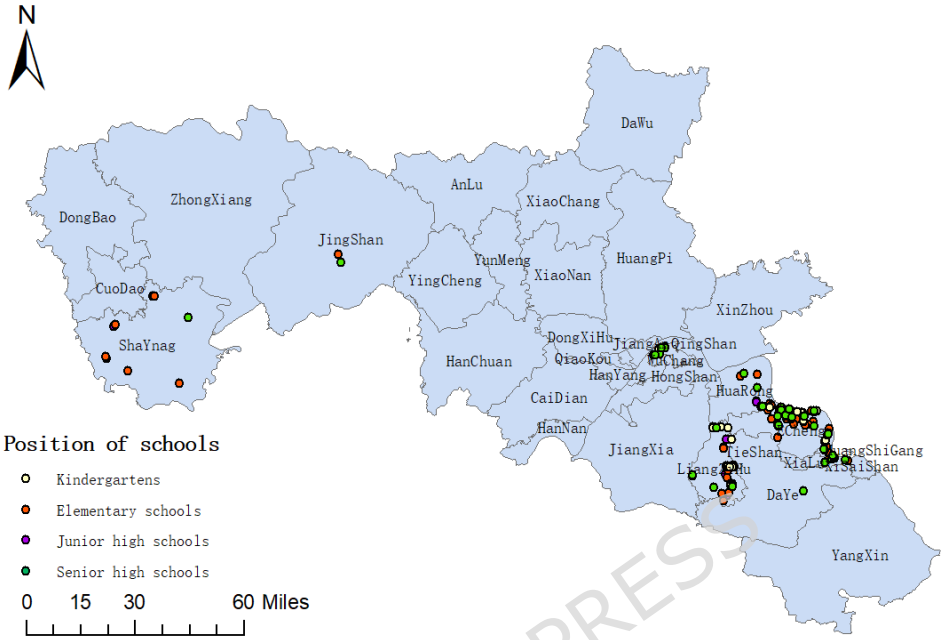

Figure 3. Locations of studied schools. Administrative boundaries were obtained from geoBoundaries (gbOpen; CC BY 4.0) for China (CHN). The ADM2 boundary layer was clipped to Hubei Province using the ADM1 boundary. The school locations were mapped using the authors' school coordinate dataset and categorized by education stage. The map was produced using QGIS software (https://qgis.org/en/site/forusers/download.html, version 3.34.8).

3.2 School models

We used non-parametric Spearman correlation analysis and linear regression models to assess the relationship between environmental factors and myopia progression. Model 1 and Model 2 represent the regression models that include all schools and exclude high schools in Table 3, respectively. The VIF values of all the factors were lower than 3 in the linear regression models,

indicating that multicollinearity of these factors can be ignored. The AIC value of Model 1 was higher than that of Model 2, indicating that the regression model excluding high schools fits better. The Spearman correlation coefficients between the 5,000-m VGI buffer and the prevalence of myopia in Models 1 and 2 were -0.738 ($p < 0.001$) and -0.334 ($p < 0.001$), respectively. Comparatively, there was no significant difference in the correlations between all NDVI buffer radii and the prevalence of myopia ($p > 0.05$). There was also no correlation between VGI and NDVI at each buffer radius ($p > 0.05$). Table 3 shows that the partial correlation coefficients between the VGI within 5,000-m buffer zone and myopia rate in Models 1 and 2 were -0.343 ($P = 0.038$) and -0.326 ($P < 0.001$), respectively. The partial correlation coefficient between the VGI within 1,000-m buffer zone and myopia rate in Model 1 was -0.217 ($P < 0.050$). Model 2 also demonstrated significant associations between myopia and both the sunshine hours and PM2.5 levels (Table 3, $P< 0.050$, $P < 0.001$). Table S1 showed that every 0.1 unit increase in VGI within the 5,000-m buffer was associated with an absolute decrease in myopia prevalence of 2.06% in Model 1 and 1.90% in Model 2 (Table S1, β=-0.206 and -0.190, respectively).

Table 3. Linear regression results for Models 1 and 2.

	Model 1		Model 2	
	Pcc (95% CI)	P	Pcc (95% CI)	P
VGI: 1,000-m buffer	-0.160 (-0.320, 0.009)	0.063	-0.217*(-0.412, -0.003)	0.047

3,000-m buffer	-0.183 (-0.369, -0.017)	0.073	-0.001 (-0.173 0.171)	0.991
5,000-m buffer	-0.343* (-0.600, -0.021)	0.038	-0.326*(-0.492, -0.137)	0.001
NDVI: 1,000-m buffer	0.146 (-0.024, 0.307)	0.091	0.139(-0.078, 0.343)	0.207
3,000-m buffer	0.234 (-0.026, 0.464)	0.076	0.049 (-0.165, 0.258)	0.655
5,000-m buffer	0.219 (-0.020, 0.435)	0.072	0.073 (-0.142, 0.282)	0.508
Carbon monoxide	0.197 (-0.025, 0.401)	0.081	0.116 (-0.102, 0.324)	0.295
PM2.5	0.060 (-0.109, 0.226)	0.487	0.212* (0.008, 0.399)	0.042
Sulfur dioxide	0.218 (-0.009, 0.424)	0.061	-0.060 (-0.272, 0.158)	0.590
Nitrogen dioxide	-0.246 (-0.476, 0.016)	0.064	0.040 (-0.176, 0.252)	0.718

Ozone	0.355 (-0.013, 0.638)	0.059	-0.005 (-0.213, 0.203)	0.963
Sunshine hours	-0.165* (-0.259, -0.067)	0.001	-0.219* (-0.414, -0.005)	0.045
Temperature	0.280 (-0.048, 0.554)	0.091	-0.111 (-0.318, 0.106)	0.315
Rainfall	0.177 (-0.014, 0.356)	0.069	0.042 (-0.175, 0.255)	0.706
Sports area	0.028 (-0.142, 0.197)	0.748	0.108 (-0.110, 0.316)	0.330
Akaike information criterion	651.24		597.54	

Model 1 is for all schools and Model 2 is for schools excluding high schools. Pcc denotes partial correlation coefficients controlling for all other environmental variables shown in the table; 95% CI was obtained by inverting the two-sided t test for partial correlation (equivalently Fisher's z with degrees-of-freedom consistent with the p-value. VGI: Vision Greenness Index; NDVI: Normalized Difference Vegetation Index. "*" $P < 0.050$.

3.3 Grade-level model

In Table 4, Models 3, 4, and 5 represent the regression models that include all kindergartens, elementary schools, and high schools, respectively. In Model 3, the partial correlation coefficient between the VGI within a 5,000-m buffer zone and the kindergarten myopia rate was -0.675 (P = 0.029), while the partial correlation coefficient between the NDVI within a 5,000-m buffer zone and the kindergarten myopia rate was -0.380 (P = 0.032). In Model 4, the partial correlation coefficient between the VGI within a 5,000-m buffer zone and the elementary school myopia rate was -0.310 (P = 0.027), while the partial correlation coefficient between the NDVI within a 5,000-m buffer zone and the elementary school myopia rate was -0.088 (P = 0.043). In kindergarten and elementary school, the partial correlation coefficients between the VGI within a 5,000-m buffer zone and myopia were more significant than those of NDVI within the same buffer zone. Model 5 did not demonstrate any correlations between the identified factors and the prevalence of myopia during high school. Table S1 showed that every 0.1 unit increase in VGI within the 5,000 m buffer was associated with an absolute decrease in myopia prevalence of 1.93% in Model 3 and 1.80% in Model 4 (Table S1, β= -0.193 and -0.180, respectively). Regarding the NDVI within the 5,000 m buffer, every 0.1 unit increase was associated with an absolute decrease in myopia prevalence of 1.04% in Model 3 and 0.24% in Model 4 (Table S1, β= -0.104 and -0.024, respectively).

Table 4. Linear regression results for Models 3, 4, and 5.

	Model 3	Model 4	Model 5

	Pcc (95% CI)	P	Pcc (95% CI)	P	Pcc (95% CI)	P
VGI: 1,000-m buffer	-0.505 (-0.817, 0.035)	0.064	-0.121 (-0.403, 0.182)	0.433	-0.346 (-0.632, 0.023)	0.065
3,000-m buffer	-0.313 (-0.605, 0.053)	0.092	-0.109 (-0.393, 0.194)	0.480	-0.135 (-0.422, 0.176)	0.393
5,000-m buffer	-0.675* (-0.860, -0.331)	0.001	-0.310* (-0.539, -0.038)	0.027	0.377 (-0.042, 0.682)	0.074
NDVI: 1,000-m buffer	0.377 (-0.757, 0.945)	0.640	-0.188 (-0.459, 0.115)	0.222	0.196 (--0.115, 0.472)	0.214
3,000-m buffer	-0.311 (-0.604, 0.055)	0.094	-0.310 (-0.583, 0.026)	0.072	0.425 (-0.052, 0.744)	0.075
5,000-m buffer	-0.380* (-0.651, -0.023)	0.038	-0.088* (-0.173, -0.002)	0.046	0.215 (-0.095, 0.487)	0.173

Carbon monoxide	-0.133 (-0.471, 0.239)	0.485	0.328 (-0.011, 0.600)	0.060	0.142 (-0.169, 0.487)	0.368
PM2.5	0.343 (-0.020, 0.626)	0.064	0.173 (-0.131, 0.447)	0.263	0.464 (-0.063, 0.789)	0.082
Sulfur dioxide	0.302 (-0.065, 0.597)	0.105	0.142 (-0.162, 0.421)	0.359	-0.245 (-0.511, 0.064)	0.117
Nitrogen dioxide	0.423 (-0.055, 0.743)	0.080	0.360 (-0.023, 0.651)	0.066	0.054 (-0.254, 0.352)	0.733
Ozone	-0.231 (-0.546, 0.141)	0.220	0.039 (-0.261, 0.332)	0.801	-0.177 (-0.456, 0.134)	0.262
Sunshine hours	-0.434 (-0.757, 0.059)	0.078	-0.369 (-0.672, 0.040)	0.074	-0.276 (-0.535, 0.030)	0.076
Temperature	-0.316 (-0.607, 0.050)	0.089	-0.037 (-0.334, 0.266)	0.813	0.028 (-0.278, 0.329)	0.861

Rainfall	0.245 (-0.126, 0.556)	0.191	-0.255 (-0.513, 0.045)	0.095	0.165 (-0.146, 0.447)	0.295
Sports area	0.369 (-0.005, 0.652)	0.054	-0.027 (-0.318, 0.269)	0.860	0.043 (-0.264, 0.342)	0.786
Akaike Information Criterion	443.72		424.12		598.45	

Model 3 is for kindergarten; Model 4 is for elementary schools; Model 5 is for high schools. Pcc denotes partial correlation coefficients controlling for all other environmental variables shown in the table; 95% CI was obtained by inverting the two-sided t test for partial correlation (equivalently Fisher's z with degrees-of-freedom consistent with the p-values. VGI: Vision Greenness Index; NDVI: Normalized Difference Vegetation Index. "*" P< 0.050.

4. Discussion

This work included 69,051 school-aged children from five cities in Hubei Province and examined environment factors around the schools, mainly comparing the relationship of two greenness exposure indices on school myopia prevalence. VGI showed a negative correlation with myopia prevalence, whereas NDVI did not, suggesting it is a better metric for assessing the influence of green spaces on myopia development than top-down satellite

products. Green spaces were only negatively related to school myopia prevalence among children in kindergarten and elementary school within a 5,000-m radius around the school. Other environmental factors, like PM2.5 and sunshine hours, were also associated with school myopia. These findings may provide a more accurate insight into the relationships between the school environment on myopia prevalence and suggest a new angle for researching greenness exposure in myopia studies.

In the regression model for all schools (Model 1), the partial correlation coefficients between VGI in a 5,000-m radius and myopia were -0.3434 (P = 0.038), with NDVI in the same buffer zone showing no significant results, suggesting that VGI was more significantly related to the school myopia than NDVI (Table 3). Measurements based on street-view images and satellite images may capture different characteristics of the green space (32). NDVI assesses vegetation coverage in the region and does not fully represent the three-dimensionality of greenness experienced by human vision because it utilizes remote sensing images (24). In contrast, VGI quantifies the proportion of green space in street view images, which captures the three-dimensional perspective from eye level (26). Because of this difference, researchers compared these two green space measurements with different health outcomes. For instance, a study demonstrated that VGI had a more significant protective effect against mental health problems compared to NDVI (33). However, other studies have shown that NDVI seemed more correlated with cardiovascular health and obesity than VGI (34, 35). Health outcomes showed different

relationships with different measurement metrics of greenness. It has been pointed out by literature that VGI is distinct but also complementary to satellite-based green space metrics like NDVI, which align with our observation that there was also no correlation between VGI and NDVI at each buffer radius (36). Therefore, VGI can be a better proxy for greenness exposures in myopia studies.

In different grade-level models, NDVI and VGI were only significantly associated with school myopia in kindergarten and elementary school, suggesting that green spaces may be more related to school myopia during the early school ages (Table 4, $P < 0.050$, $P < 0.001$). Another study reflected these results by showing that green spaces only seem to have a protective effect before twelve years of age (37). Laboratory and epidemiologic studies show that myopia rates rapidly increase during the early school years, which also suggests that environmental prevention of school myopia is more efficient at an early age (38, 39). Our work corroborated these results. In higher-grade students, the intense academic pressure and limited outdoor time may offset the potential benefits of green space and other environmental factors (40). As such, modifying green spaces as a strategy for myopia prevention may be more efficient for kindergartens and elementary schools. We found the rapid increases in myopia rates during the third years of kindergarten and elementary school, which may be due to the sudden increase in academic pressure of entering a higher school level during these periods that leading to increased near-work time and decreased time outdoors. As such, these two time points may be critical for myopia prevention. Gaining green

spaces in the surroundings of kindergartens and elementary schools is a more cost-effective strategy for myopia prevention.

Further, green spaces were majorly associated with myopia when they were located within a 5,000-m buffer zone of schools (Table 4, $P < 0.050$, $P < 0.001$). Strength of associations between green space and health outcomes can vary depending on the spatial scale (32). Variations in the correlation between these factors may arise from differences in the availability, accessibility, and utilization of green spaces (41). In Shenzhen and Beijing, green spaces within 500-m of schools were associated with a reduced risk for myopia (14, 21). In contrast, green spaces within 5,000-m of schools provided protective effects in Wuhan (13). A 5,000-m radius may represent the area around which students participate in after-school activities in Hubei province. This area is wider than that observed in Shenzhen and Beijing, and may be due to differences in city planning and urban environment. As such, to focus on the impact of environmental factors more precisely, this study employs a spatial research approach grounded in regional clustering characteristics. We selected schools from five cities located in mountain areas, riverside areas, lakeside areas, and mixed-terrain areas in Hubei. This clustering aimed to better explore the effects of environmental factors among multiple regions, thereby representing the association between green spaces and myopia for Hubei province as a whole.

The potential protective effect of green spaces against myopia may be explained by several mechanisms. A common hypothesis is that

more greenness is associated with more time outdoors (42). Increased outdoor time promotes distance vision, which reduces myopia. Increased outdoor time also implies less indoor, screen, and near-work time, which in turn reduces myopia progression (43). Previous mediation analysis also supported this hypothesis by suggesting that the effect of school-based green space on myopia was mediated by outdoor time (40). A greener environment also provides higher spatial frequencies than indoor settings, which have been shown to influence ocular growth regulation mediated by retinal dopamine to inhibit axial growth and the onset of myopia (44, 45). Our study also found that sunshine hours were negatively related to myopia (Table 3, $P < 0.050$). Sunlight exposure may stimulate dopamine release in the retina, which inhibits axial length elongation and reduces myopia progression (46). PM2.5 was also found to be positively related to myopia (Table 3, $P < 0.050$). Air pollution exposure, measured through PM2.5 concentrations, may increase ocular inflammation, resulting in retinal ischemia, which promotes myopia progression (47). City planning for myopia prevention may benefit from a clearer understanding of how environmental factors influence myopia progression.

A comprehensive understanding of the relationship between environmental factors and myopia across diverse regions is necessary for making effective myopia prevention strategies. Although interventions such as orthokeratology lenses, lenses that impose myopic defocus, red light therapy, and low-dose atropine have demonstrated efficacy in controlling myopia progression, their widespread application is limited by cost and adherence challenges

(48-50). According to a nationwide cost-of-illness study, the total number of myopic people in China was estimated to be 143.6 million, and the cost per person was approximated at 69 US dollars, which may be prohibitive for poorer populations (6). Population-based strategies like city planning may be more feasible and cost-effective (51). China recently committed to prioritizing student health and welfare by enforcing population-based myopia prevention strategies (52). Improving living conditions and urban planning may be a promising myopia prevention strategy (53). As previously mentioned, environmental risk factors vary across different regions. Detailed surveys of diverse regions may reveal other environmental risk factors that influence myopia progression. Regions with high myopia prevalence may benefit from landscape redesigns and school renovations to reduce the onset and progression of the disease. Studies like these ultimately aim to contribute to affordable and effective population-based myopia control strategies.

This study is limited by first, VGI for each location was obtained by averaging greenness values from four cardinal directions. Averaging may obscure directional variability in green space exposure due to projection differences. Although previous studies showed that spatial heterogeneity of street-view green space is mainly derived from land cover and landscape pattern but not photographic directional variability, future work could compare the four direction values and, where necessary, apply orientation-weighted or direction-specific exposure models according to participants' mobility path (54, 55). Second, VGI with the radii of

1,000-m, 3,000-m, and 5,000-m were calculated to evaluate the street-view green space in different buffer zones around the school. Images in the schools were unavailable to obtain, inhibiting the assessment of visual greenness within the buffer zone smaller than 1,000-m. Future studies may need to acquire images in the school to assess visual greenness with smaller buffer zones and include school areas. Third, differences in green space between summer and winter may not adequately be represented in this study and affect our results. However, this difference was actually not significant, as the semantic segmentation algorithm does not purely depend on the greenness of leaves but on the characteristics of vegetation itself. Fourth, this study assessed environment exposure based on school locations rather than individual trajectories to explore the relationship between myopia prevalence and the surrounding school environment. Some research used wearable devices with GPS tracking, which may provide a more personalized exposure assessment (56,57). Based on the school-level exposure results, future work may benefit from incorporating GPS data to give the exposure assessment of individual activity. Lastly, this study was a cross-sectional study, which cannot establish causal relationships between the examined environmental factors and myopia rates. Due to data availability and privacy constraints, we could not adjust for some individual-level confounders such as socioeconomic status (SES) and parental myopia. Future interventional and longitudinal studies are needed to incorporate a broader range of confounders from reliable resources and assess the mediation effect of these factors.

5. Conclusion

This cross-sectional study included 69,051 school-aged children from five cities in Hubei Province and examined the effects of green space, sunshine, and air pollution on myopia prevalence in schools. Deep learning methods were employed to calculate VGI from street view images. We innovatively compared this eye-level greenness exposure index with NDVI and revealed a stronger association between VGI and myopia. Green space exhibited a protective association with myopia among early school-age children within a 5,000-m radius, suggesting enlarging and optimizing green spaces around kindergarten and elementary schools and across a broader range as an efficient strategy for myopia prevention. These findings provide a clearer insight into how the green space and other identified factors impact school myopia.

Abbreviations

NDVI: Normalized Difference Vegetation Index; VGI: Vision Greenness Index; VIF: Variance inflation factor; AIC: Akaike Information Criterion.

Declarations

Ethics approval and consent to participate

The study was approved by the Ethics Committee of Renmin Hospital of Wuhan University (WDRY2020-K234) and followed the tenets of the Declaration of Helsinki. Informed consent was obtained from all the subjects in this study.

Consent for publication

Not applicable.

Availability of data and materials

The data that has been used is commonly confidential. The parameters in our model (text, tables, figures, models, and appendices) are only available on reasonable request from the author Dihao Hua (Email: dihaohuaphd@163.com) under certain conditions, with the consent of all participating centers and with a signed data access agreement.

Competing interests

The authors declare no conflicts of interest.

Funding

National Natural Science Foundation of China (NO. 42201457)

Authors' contributions

Conceptualization, D.H.; Writing–original draft preparation, D.H., T.Y., C.Q., J.Z.; Writing—review and editing, Z.Y., Y.X., C.C, and Z.C.; Funding acquisition, D.H.; Visualization, D.H., T.Y., C.Q.; Resources, D.H., J.Z., G.L., A.S., W.S., M.M.; Investigation, F.Z., R.Z. All the authors have read and agreed to the published version of the manuscript.

Acknowledgments

Not applicable.

Reference

1. Morgan IG, Ohno-Matsui K, Saw SM. Myopia. *Lancet.* 379(9827):1739-48. 10.1016/s0140-6736(12)60272-4 (2012)

2. Holden BA, et al. Global Prevalence of Myopia and High Myopia and Temporal Trends from 2000 through 2050. *Ophthalmology*.123(5):1036-42. 10.1016/j.ophtha.2016.01.006 (2016)

3. Hu Y, Ding X, Guo X, Chen Y, Zhang J, He M. Association of Age at Myopia Onset with Risk of High Myopia in Adulthood in a 12-Year Follow-up of a Chinese Cohort. JAMA Ophthalmol.138(11):1129-34. 10.1001/jamaophthalmol.2020.3451 (2020)

4. Jonas JB, Wang YX, Dong L, Panda-Jonas S. High Myopia and Glaucoma-Like Optic Neuropathy. *Asia-Pacific journal of ophthalmology (Philadelphia, Pa)* 9(3):234-8. 10.1097/apo.0000000000000288 (2020)

5. Haarman AEG, Enthoven CA, Tideman JWL, Tedja MS, Verhoeven VJM, Klaver CCW. The Complications of Myopia: A Review and Meta-Analysis. Investigative ophthalmology & visual science. 61(4):49. 10.1167/iovs.61.4.49. (2020)

6. Ma Y. et al. Healthcare Utilization and Economic Burden of Myopia in Urban China: A Nationwide Cost-of-Illness Study. *Journal of global health.*12:11003. 10.7189/jogh.12.11003 (2022)

7. Naidoo KS. et al. Potential Lost Productivity Resulting from the Global Burden of Myopia: Systematic Review, Meta-Analysis, and Modeling. *Ophthalmology*. 126(3):338-46. 10.1016/j.ophtha.2018.10.029 (2019)

8. Li R. et al. Implementing a Digital Comprehensive Myopia Prevention and Control Strategy for Children and Adolescents in

China: A Cost-Effectiveness Analysis. *The Lancet regional health Western Pacific*. 38:100837. 10.1016/j.lanwpc.2023.100837 (2023)

9. Morgan IG, Wu PC, Ostrin LA, Tideman JWL, Yam JC, Lan W, et al. Imi Risk Factors for Myopia. *Investigative ophthalmology & visual science* 62(5):3. 10.1167/iovs.62.5.3 (2021)

10. Choi KY, Chan SS, Chan HH. The Effect of Spatially-Related Environmental Risk Factors in Visual Scenes on Myopia. *Clinical & experimental optometry.* 105(4):353-61. 10.1080/08164622.2021.1983400 (2022)

11. Eppenberger LS, Sturm V. The Role of Time Exposed to Outdoor Light for Myopia Prevalence and Progression: A Literature Review. *Clinical ophthalmology (Auckland, NZ)*. 14:1875-90. 10.2147/opth.S245192 (2020)

12. Yuan T, Zou H. Effects of Air Pollution on Myopia: An Update on Clinical Evidence and Biological Mechanisms. *Environmental science and pollution research international*. 29(47):70674-85. 10.1007/s11356-022-22764-9 (2022)

13. Cui Q. et al. Impacts of Environments on School Myopia by Spatial Analysis Techniques in Wuhan. *Sci Rep.* 14(1):29941. 10.1038/s41598-024-81270-9 (2024)

14. Zhang C, Wang C, Guo X, Xu H, Qin Z, Tao L. Effects of Greenness on Myopia Risk and School-Level Myopia Prevalence among High School-Aged Adolescents: Cross-Sectional Study. *JMIR public health and surveillance.* 9:e42694. 10.2196/42694 (2023)

15. Lu C. et al. Socioeconomic Disparities and Green Space Associated with Myopia among Chinese School-Aged Students: A Population-Based Cohort Study. *Journal of global health.*14:04140 10.7189/jogh.14.04140 (2024)

16. Zhao, L. et al. Prevalence and risk factors of myopia among children and adolescents in Hangzhou. *Scientific Reports* 14, 24615, doi:10.1038/s41598-024-73388-7 (2024).
17. Clark, R. et al. Time Spent Outdoors Partly Accounts for the Effect of Education on Myopia. Investigative ophthalmology & visual science 64, 38, doi:10.1167/iovs.64.14.38 (2023).
18. Nguyen PY, Astell-Burt T, Rahimi-Ardabili H, Feng X. Green Space Quality and Health: A Systematic Review. *International journal of environmental research and public health.* 18(21). 10.3390/ijerph182111028 (2021)
19. Rahimi-Ardabili H. et al. Green Space and Health in Mainland China: A Systematic Review. *International journal of environmental research and public health*. 18(18). 10.3390/ijerph18189937 (2021)
20. Yang Y, Liao H, Zhao L, Wang X, Yang X, Ding X, et al. Green Space Morphology and School Myopia in China. *JAMA Ophthalmol.* 142(2):115-22. 10.1001/jamaophthalmol.2023.6015 (2024)
21. Yang BY. et al. Greenness Surrounding Schools and Visual Impairment in Chinese Children and Adolescents. *Environmental health perspectives.* 129(10):107006. 10.1289/ehp8429 (2021)
22. Yang Y. et al. Spatial Technology Assessment of Green Space Exposure And myopia. *Ophthalmology.* 129(1):113-7. 10.1016/j.ophtha.2021.07.031 (2022)
23. Martinez AI, Labib SM. Demystifying Normalized Difference Vegetation Index (Ndvi) for Greenness Exposure Assessments and Policy Interventions in Urban Greening. *Environ Res.* 220:115155. 10.1016/j.envres.2022.115155 (2023)
24. Larkin A, Hystad P. Evaluating Street View Exposure Measures of Visible Green Space for Health Research. *Journal of exposure*

science & environmental epidemiology. 29(4):447-56. 10.1038/s41370-018-0017-1 (2019)

25. Labib SM, Huck JJ, Lindley S. Modelling and Mapping Eye-Level Greenness Visibility Exposure Using Multi-Source Data at High Spatial Resolutions. *Science of The Total Environment*. 755. https://doi.org/10.1016/j.scitotenv.2020.143050 (2021)
26. Shi X, Zhang F, Chipman JW, Li M, Khatchikian C, Karagas MR. Measuring Greenspace in Rural Areas for Studies of Birth Outcomes: A Comparison of Street View Data and Satellite Data. *GeoHealth.* 8(4):e2024GH001012. 10.1029/2024gh001012 (2024)
27. Helbich M, Yao Y, Liu Y, Zhang J, Liu P, Wang R. Using Deep Learning to Examine Street View Green and Blue Spaces and Their Associations with Geriatric Depression in Beijing, China. *Environment International.* 126:107-17. 10.1016/j.envint.2019.02.013 (2019)
28. Wang R. et al. Exploring the Impacts of Street-Level Greenspace on Stroke and Cardiovascular Diseases in Chinese Adults. *Ecotoxicology and Environmental Safety.* 243. 10.1016/j.ecoenv.2022.113974 (2022)
29. Flitcroft DI. et al. Imi - Defining and Classifying Myopia: A Proposed Set of Standards for Clinical and Epidemiologic Studies. *Investigative ophthalmology & visual science.* 60(3):M20-m30. 10.1167/iovs.18-25957 (2019)
30. Martinez-Sanchez L, Hufkens K, Kearsley E, Naydenov D, Czúcz B, van de Velde M. Semantic Segmentation Dataset of Land Use/Cover Area Frame Survey (Lucas) Rural Landscape Street View Images. *Data in brief*. 54:110394. 10.1016/j.dib.2024.110394 (2024)

31. Pan W. Akaike's Information Criterion in Generalized Estimating Equations. *Biometrics*. 57(1):120-5. 10.1111/j.0006-341x.2001.00120.x (2001)
32. Labib SM, Lindley S, Huck JJ. Spatial Dimensions of the Influence of Urban Green-Blue Spaces on Human Health: A Systematic Review. *Environmental Research.* 180:108869. 10.1016/j.envres.2019.108869 (2020)
33. Wang R, Feng Z, Pearce J, Liu Y, Dong G. Are Greenspace Quantity and Quality Associated with Mental Health through Different Mechanisms in Guangzhou, China: A Comparison Study Using Street View Data. *Environmental pollution* (Barking, Essex : 1987). 290:117976. 10.1016/j.envpol.2021.117976 (2021)
34. Yi L. et al. Satellite-Based and Street-View Green Space and Adiposity in Us Children. *JAMA network open.* 7(12):e2449113. 10.1001/jamanetworkopen.2024.49113 (2024)
35. Yi L. et al. Assessing Greenspace and Cardiovascular Health through Deep-Learning Analysis of Street-View Imagery in a Cohort of Us Children. *Environ Res.* 265:120459. 10.1016/j.envres.2024.120459 (2025)
36. Kumakoshi Y, Chan SY, Koizumi H, Li X, Yoshimura Y. Standardized Green View Index and Quantification of Different Metrics of Urban Green Vegetation. 12(18):7434. (2020)
37. Peng BA, Naduvilath TJ, Flitcroft DI, Jong M. Is Myopia Prevalence Related to Outdoor Green Space? *Ophthalmic and Physiological Optics.* 41(6):1371-81. 10.1111/opo.12896 (2021)
38. Morgan IG, He M, Rose KA. Epidemic of Pathologic Myopia: What Can Laboratory Studies and Epidemiology Tell Us? *Retina*

(Philadelphia, Pa). 37(5):989-97. 10.1097/iae.0000000000001272 (2017)

39. Rose KA, French AN, Morgan IG. Environmental Factors and Myopia: Paradoxes and Prospects for Prevention. *Asia-Pacific journal of ophthalmology (Philadelphia, Pa).* 5(6):403-10. 10.1097/apo.0000000000000233 (2016)

40. Wang, J. et al. Outdoor Time Could Regulate the Effects of Green Environment on Myopia in Chinese Children and Adolescents. Ophthalmic epidemiology, 1-10, doi:10.1080/09286586.2025.2475207 (2025).

41. Fernandes A. et al. Availability, Accessibility, and Use of Green Spaces and Cognitive Development in Primary School Children. Environmental Pollution (2023) 334:122143. https://doi.org/10.1016/j.envpol.2023.122143.

42. Wang J. et al. Association of Built Environment Attributes with Screening Myopia among Children and Adolescents: Large-Sample, Cross-Sectional, Observational Evidence from Shanghai, China. *SSRN Electronic Journal*. 10.2139/ssrn.4124055 (2022)

43. Huang L. et al. Association between Greater Residential Greenness and Decreased Risk of Preschool Myopia and Astigmatism. *Environmental Research* 196:110976. 10.1016/j.envres.2021.110976 (2021)

44. Flitcroft DI, Harb EN, Wildsoet CF. The Spatial Frequency Content of Urban and Indoor Environments as a Potential Risk Factor for Myopia Development. *Investigative ophthalmology & visual science.* 61(11):42. 10.1167/iovs.61.11.42 (2020)

45. Li DL, Dong XX, Yang JL, Lanca C, Grzybowski A, Pan CW. Lower Indoor Spatial Frequency Increases the Risk of Myopia in

Children. *The British journal of ophthalmology*. 10.1136/bjo-2024-325888 (2024)

46. Wu P-C. et al. Myopia Prevention and Outdoor Light Intensity in a School-Based Cluster Randomized Trial. *Ophthalmology.* 125(8):1239-50. 10.1016/j.ophtha.2017.12.011 (2018)

47. Wei CC. et al. Pm2.5 and Nox Exposure Promote Myopia: Clinical Evidence and Experimental Proof. *Environmental pollution*. 254(Pt B):113031. 10.1016/j.envpol.2019.113031 (2019)

48. Cho P, Tan Q. Myopia and Orthokeratology for Myopia Control. *Clinical & experimental optometry.* 102(4):364-77. 10.1111/cxo.12839 (2019)

49. Jiang DD, Zhao CP, Ding WZ, Leng L. The Role of Peripheral Retinal Defocus in Myopia Progression. *Chinese journal of ophthalmology.* 60(6):541-6. 10.3760/cma.j.cn112142-20231024-00173 (2024)

50. Jiang Y. et al. Effect of Repeated Low-Level Red-Light Therapy for Myopia Control in Children: A Multicenter Randomized Controlled Trial. Ophthalmology (2022) 129(5):509-19. https://doi.org/10.1016/j.ophtha.2021.11.023.

51. Morgan IG, Jan CL. China Turns to School Reform to Control the Myopia Epidemic: A Narrative Review. *Asia-Pacific journal of ophthalmology (Philadelphia, Pa).* 11(1):27-35. 10.1097/apo.0000000000000489 (2022)

52. Morgan IG, Lan W. New Clinical and Public Health Perspectives on Myopia Prevention and Control in China. *Eye (London, England).* 38(1):8-9. 10.1038/s41433-023-02625-6 (2024)

53. Zhu Z, Chen Y, Tan Z, Xiong R, McGuinness MB, Müller A. Interventions Recommended for Myopia Prevention and Control

among Children and Adolescents in China: A Systematic Review. *The British journal of ophthalmology.* 107(2):160-6. 10.1136/bjophthalmol-2021-319306 (2023)

54. Wang R, Feng Z, Pearce J, Zhou S, Zhang L, Liu Y. Dynamic Greenspace Exposure and Residents' Mental Health in Guangzhou, China: From over-Head to Eye-Level Perspective, from Quantity to Quality. *Landscape and urban planning* 215:104230. 10.1016/j.landurbplan.2021.104230 (2021)

55. Zhang W, Zeng H. Spatial Differentiation Characteristics and Influencing Factors of the Green View Index in Urban Areas Based on Street View Images: A Case Study of Futian District, Shenzhen, China. *Urban Forestry & Urban Greening.* 93:128219. 10.1016/j.ufug.2024.128219 (2024)

56. Gibaldi, A., Harb, E. N., Wildsoet, C. F. & Banks, M. S. A Child-Friendly Wearable Device for Quantifying Environmental Risk Factors for Myopia. *Translational vision science & technology* 13, 28, doi:10.1167/tvst.13.10.28 (2024).

57. Wen, L. et al. The Clouclip, a wearable device for measuring near-work and outdoor time: validation and comparison of objective measures with questionnaire estimates. *Acta ophthalmologica* 99, e1222-e1235, doi:10.1111/aos.14785 (2021).